Quantum Information Processing using Pulsed NMR

Joan C. Smith[*]
MIT Department of Physics
(Dated: March 15, 2011)

This experiment demonstrates the use of pulsed NMR to implement a two qubit quantum computer. Pulsed NMR is performed on a 7% ^{13}CHCl$_3$ (chloroform) sample. The hydrogen and carbon nuclei in the sample have different Larmor frequencies, allowing the nucleons to be independently rotated. Quantum operations are performed by applying series of rotations to the each qubit. Pure initial states are constructed using temporal averaging on the thermal state of the system. The thermal state ratio of peak integrals deviate from the expected theoretical thermal values state by 1.5% and the pure state ratios differ by 20%. The pure initial states are used to demonstrate a CNOT gate that differs from the theoretical peak integral ratios by 20%. Using the CNOT gate, the Deutsch-Jozsa algorithm for determining balance of a single-bit function is performed for each of the four possible logical functions. The Deutsch-Jozsa algorithm is shown to behave as theoretically predicted.

1. INTRODUCTION

This experiment demonstrates the pulsed NMR method for performing quantum calculations on two qubits. Pulsed NMR is performed independently on ensembles of hydrogen and carbon nuclei[1] within a sample of chloroform. Hydrogen and carbon nuclei ensembles are manipulated first into the four possible pure states. Once the pure states have been obtained, quantum operations are performed to demonstrate logic gates. The logic gates are combined to execute the Deutsch-Jozsa algorithm. The Deutsch Jozsa algorithm is provably faster than its classical counterpart.

2. CLASSICAL AND QUANTUM COMPUTING

Classical computations are performed using electrical pulses. The pulses are sent through circuitry that can produce either on or off signals based on the input. The on and off signals represent bits. In quantum computing, bits are replaced with qubits. Instead of on and off electrical pulses, qubits are the spins of molecules. This experiment demonstrates a two qubit quantum computer. To introduce the notation, wavefunctions of the two qubits will be represented as the ket $|HC\rangle$. NMR is used to manipulate the spin of the hydrogen and carbon nuclei. Since protons are spin $\frac{1}{2}$ particles, each of the two qubits can be either in a $+\frac{1}{2}$ state, a $-\frac{1}{2}$ state, or a superpostition of the two. Superposition states are not observable in this experiment, so the two observable states will be represented as 0 and 1 respectively. There are four possible pure states for the system, $|00\rangle$, $|01\rangle$, $|10\rangle$, and $|11\rangle$[2], but many other mixed states. Producing pure states from the thermal initial state is the first experimental Quantum logic operations are performed only pure states to produce meaningful results.

2.1. Rotation Matrices for Quantum Logic Gates

In this experiment, nuclear magnetic resonance is used to perform operations, so the operations are rotations. Performing rotations about the $\hat{x}$, $\hat{y}$ and $\hat{z}$ axes on the state $|00\rangle$ allows the creation of of the remaining three pure states. The method for obtaining the state $|00\rangle$ will be discussed in Sec. 4.

The state $|00\rangle$ is the matrix with a 1 in the the top-leftmost entry of a 4x4 density matrix. A rotation matrix, like

$$R_{y1}(\pi) = \frac{1}{2}\begin{pmatrix} 1 & -1 & 0 & 0 \\ 1 & 1 & 0 & 0 \\ 0 & 0 & 1 & -1 \\ 0 & 0 & 1 & 1 \end{pmatrix}^2 \tag{1}$$

can be used to modify a state. For example,

$$R_{y1}(\pi)|00\rangle = |01\rangle \tag{2}$$

$R_{y1}(\pi)$ means a rotation about the $\hat{y}$ axis on the carbon nuclei, of π radians. Using similar rotation matrices other, and more interesting computations can be performed.

2.2. Quantum Mechanical System

The Hamiltonian for the two qubit quantum system is

$$H = \frac{\hbar}{4}J\sigma_z^1\sigma_z^2 + \frac{\hbar P_{x1}(t)}{2}\sigma_x^1 + \frac{\hbar P_{y1}(t)}{2}\sigma_y^1 + \frac{\hbar P_{x2}(t)}{2}\sigma_x^2 + \frac{\hbar P_{y2}(t)}{2}\sigma_y^2 \tag{3}$$

Here the $P(t)$ terms are classical terms that control a single qubit each, and the $J\sigma_z^1\sigma_z^2$ term is the spin-spin coupling. The the $P(t)$ terms are turned off during free evolution, leaving the $J\sigma_z^1\sigma_z^2$ term to dominate. When single qubit rotations are performed the appropriate $P(t)$ term is taken to be much larger than J, such that the interaction term can be neglected.

———————
[*]Electronic address: joans@mit.edu

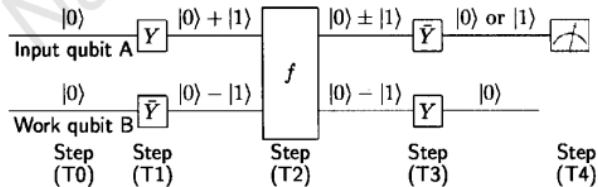| In		Out	
H	C	H	C
0	0	0	0
0	1	0	1
1	0	1	1
1	1	1	0

TABLE I: Truth table for quantum CNOT gate

FIG. 1: The block diagram for the Deutsch-Jozsa algorithm. Unlike an equivalent classical computing algorithm to perform the same function, the Deutsch-Jozsa algorithm requires only one evaluation of the input function. This diagram is taken from Chuang. [3]

2.2.1. CNOT Gate

One of the quantum operations is CNOT. A CNOT operation is similar to a classical XOR. XOR, represented by $\oplus$, is 0 if two input bits are the same, and one if the input bits are different. The quantum cnot similarly takes two bits as input, but it produces two output bits. The truth table for CNOT is shown in Tab. 2.2.1. A quantum cnot is performed with a series of rotations that can be calculated. CNOT was determined to be

$$
\begin{aligned}
U_{CNOT} &= R_{x1}(\pi)R_{y1}(\pi)R_{x1}(\frac{\pi}{2})R_{y1}(-\frac{\pi}{2}) \\
&\quad R_{y2}(\frac{\pi}{2})R_{x2}(\frac{\pi}{2})R_{y2}(-\frac{\pi}{2})\tau R_{x1}(\pi)R_{y1}(\frac{\pi}{2}).
\end{aligned}
$$

Where τ is the delay in milliseconds for which the system is allowed to undergo free evolution. During this time, the spin-spin interaction term of the Hamiltonian, Eq. 3, dominates. The value of τ is determined by the spin-coupling constant J, introduced above. Its value is $\tau = \frac{1}{J}$.

2.3. Deutsch Jozsa Algorithm

The Deutsch-Jozsa algorithm was one of the first algorithms that is provably faster than an equivalent classical computing algorithm. It is a method to evaluate whether a given single bit function is balanced or constant. As in the classical method, the Deutsch-Jozsa algorithm evaluates $f(0) \oplus f(1)$. If the function is constant $f(0)$ and $f(1)$ will have the same value, so the XOR operation will

produce a 0. If the function is balanced, then $f(0)$ and $f(1)$ will have opposite values, so the XOR produces a 1. The quantum algorithm is provably faster because it only needs to evaluate the function once. The classical method must evaluate the function twice, once for $f(0)$ and once for $f(1)$. Since there are exactly four possible functions that take a single bit as input and produce a single bit as output, the Deutsch-Jozsa can be studied and confirmed for this simplest case. The block diagram for the Deutsch-Jozsa is shown in 1.

The Deutsch-Jozsa algorithm for single qubit functions requires two qubits: one qubit as input and one to evaluate with. During execution both bits are changed. The input qubit is returned to its initial state before execution is complete. There are four steps to evaluate the algorithm. First, perform a rotation about the y axis on the input qubit to transform the state from $|00\rangle$ to $\frac{1}{\sqrt{2}}(|0\rangle + |1\rangle) \otimes |0\rangle$. Simultaneously perform a rotation by the same amount, about the $-y$ axis on the second qubit. This produces the state $\frac{1}{2}[(|0\rangle + |1\rangle) \otimes (|0\rangle - |1\rangle)]$. Next call the single qubit function, and apply it to the input qubit, add the result to the second qubit. Since the input bit is simultaneously 0 and 1, the function must only be executed once. The function must be implemented in a unitary and reversible way. This puts the system in the state $\frac{1}{2}\left[\left(-1^{f(0)}|0\rangle + -1^{f(1)}|1\rangle\right) \otimes (|0\rangle - |1\rangle)\right]$. The final step is to take the reverse transformations of those performed in the initial step. This removes the superposition for both the input bit and the second bit, leaving the system in the final state

$$
\frac{1}{2}\left[\left((-1)^{f(0)} + (-1)^{f(1)}\right)|0\rangle + \left(-(-1)^{f(0)} + (-1)^{f(1)}\right)|1\rangle\right] \otimes |0\rangle
$$
(4)

This state expresses the result of the Deutsch-Jozsa in the first qubit. If the function is constant then $(-1)^{f(0)} + (-1)^{f(1)} = \pm 2$ and $-(-1)^{f(0)} + (-1)^{f(1)} = 0$, so the resulting state is $|00\rangle$. If the function is balanced, then $-(-1)^{f(0)} + (-1)^{f(1)} = \pm 2$ and $(-1)^{f(0)} + (-1)^{f(1)} = 0$, so the resulting state is $|10\rangle$.

Implementing the pulse sequence

$$
R_{y1}R_{\bar{y}2}U_{fk}R_{\bar{y}1}R_{y2}
$$
(5)

on a state $|00\rangle$ will yield $|00\rangle$ if the function is constant and $|10\rangle$ if the function is balanced [3].

3. EXPERIMENTAL SETUP

As demonstrated above quantum operations are matrices and operators for interesting computations can be built out of rotation matrices. NMR allows the rotation of nucleon spins. A two qubit system is implemented by performing NMR on a sample that contains two distinct elements. In this case, the sample is 7% ^{13}CHCl$_3$. The sample is placed in a large homogenous magnetic field and a small oscillating rf field is applied to either nucleon. The rf pulses are applied to rotate the hydrogen
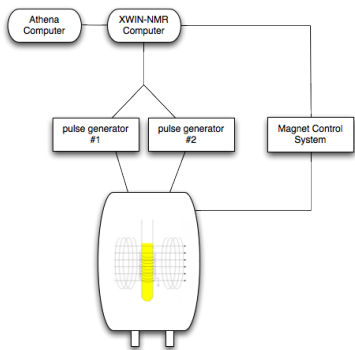
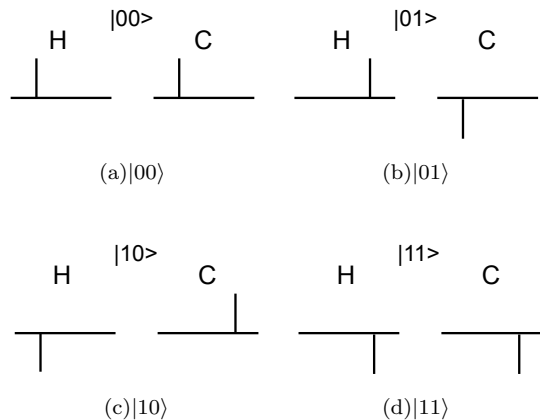FIG. 2: Experimental apparatus.

(a)|00⟩   (b)|01⟩

(c)|10⟩   (d)|11⟩

FIG. 3: Theoretically predicted pure state spectra. Readout pulses produce hydrogen peaks $a - c$ and $b - d$ and carbon peaks $a - b$ and $c - d$, where a, b, c, d are the diagonal elements of a density matrix.

and carbon nucleons independently. Measurements are Fourier transforms of the free induction decays produced in the NMR spectrometer.

3.1. Experimental Apparatus

Pulsed NMR is performed using a 200MHz Bruker NMR Spectrometer. The large magnetic field is produced by a cryomagnet cooled with both liquid hydrogen and liquid nitrogen. The magnetic field is homogenous to one part in $\frac{10^9}{cm^3}$. There are two independent pulse generators and a control system for the magnet. All three are connected to a controlling computer. Interaction with the spectrometer occurs through pulse-program scripts written in and run on Matlab.

4. DATA AND ANALYSIS

The pure states necessary to test the CNOT gate and Deutsch-Jozsa algorithm are obtained through temporal averaging. Temporal averaging requires three experiments. Each experiment is one permutation of the thermal state. Permutations are performed by acting near-CNOTs on the thermal state. Near-cnot operations are performed instead of cnots because near-cnots take less time and the phases in the permutations do not matter. The results of the three permutations are combined linearly, and this linear combination produces an effectively pure state.

State measurements are obtained by performing a readout pulse $R_x(\frac{\pi}{2})$ on each qubit. The readout pulse produces the spectra data shown in Figs. 4-7. The spin-spin coupling between the carbon and hydrogen produces two spectra peaks in each hydrogen and carbon spectrum. The distance between the two peaks is determined by J from the Hamiltonian, Eq. 3.

Each pure state was fit to a real valued Lorentzian, $f(x) = Re\left(\frac{\alpha\Gamma}{i(\omega-\omega_0)+\Gamma}\right)$. On each graph the peak integrals are shown above χ^2.
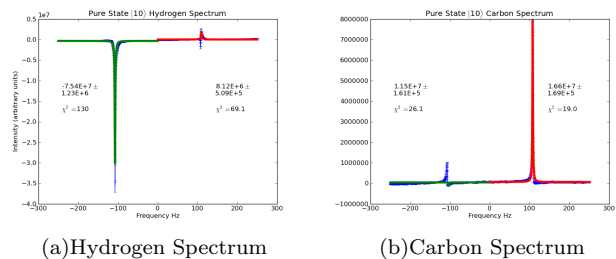

(a)Hydrogen Spectrum   (b)Carbon Spectrum

FIG. 4: Example of a pure state, $|10\rangle$. State is obtained by performing temporal averaging on the thermal state and applying a pulse $R_{x1}(\pi)$.

4.1. Calibration

Calibration of the experimental apparatus was done prior to taking each set of data. Calibrations were performed to measure 90° pulse widths for both hydrogen and carbon, phase reference angles to produce spectra with <10% imaginary components, the separation between the peaks in each spectrum (determining J), and the spin-lattice relaxation time[4] of each qubit.

90° pulse widths were determined to be $7.440 \pm .004 \mu s$ for hydrogen, and $8.200 \pm .008 \mu s$ for carbon. The errors are due to statistical error over three trials.

Pulse separation, J from Eq. 3, was measured to be $J = 216 \pm 17$Hz. This is a dominant source of error in the experiment.

Spin-lattice relaxation time was determined to be $T_1 = 17 \pm .6$ s for hydrogen and $T_1 = 12 \pm .4$s for carbon.
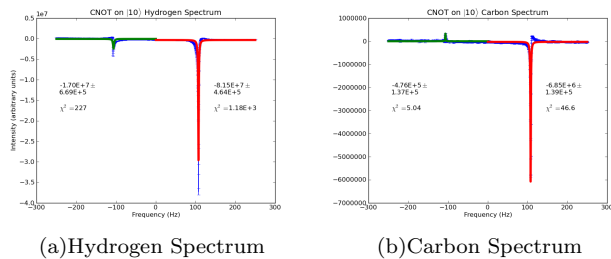
(a)Hydrogen Spectrum (b)Carbon Spectrum

FIG. 5: CNOT acting on the state $|10\rangle$. The second negative amplitude peak in both the H and C spectra indicate that the sample is in the state $|11\rangle$. This is the expected result, and support the hypothesis that CNOT can be implemented with an NMR quantum computer.

4.2. Pure States

Temporal averaging is used to effectively create the state $|00\rangle$. To obtain the states $|01\rangle$, $|10\rangle$ and $|11\rangle$ rotations are performed on the appropriate bits of the $|00\rangle$ state. The theoretically predicted expected spectra for each of the four pure states is shown in Fig. 3.

For example, to obtain the state $10\rangle$, $R_{y1}(\pi)|00\rangle = |10\rangle$. This pure state is shown in Fig. 4.

Three trials were taken for each of the four states. The statistical random error (shown as errorbars in Fig. 4) was calculated by taking the standard deviation over the three trials for each state. Systematic errors will be discussed in Sec. 4.5

4.3. CNOT

CNOT was performed on each pure state, and the expected output is shown in Tab. 2.2.1. The pulse sequence for CNOT on a state is shown in Eq. 4. For each of the four pure states, CNOT trials were run three times. Data for CNOT on $|10\rangle$ is shown in Fig. 5.

4.4. Deutsch-Jozsa Algorithm

Experiments were performed with Deutsch-Jozsa for each of the four possible logical functions. As explained above, the pulse sequence for the Deutsch-Jozsa algorithm is Eq. 5. As expected, the data obtained was

confirmed to be identical for the two constant functions, f_1 and f_2 and identical for the two balanced functions, f_3 and f_4. An example of each is shown. The constant function data is shown in Fig. 6, and the balanced function data is shown in Fig. 7. Results were found to agree with the theoretical predictions.

4.5. Sources of Error and Error Analysis

Statistical random error is shown as error bars on each graph. Fits were performed by minimizing χ^2 on the analytical Lorentzian. The most significant contribution to the statistical error is the inhomogeneity of the field applied by the rf pulses. An additional smaller contribution is made by the instability of power running the spectrometer[5].

Systematic error was accounted for by calculating the peak integrals on each of the pure state fits and then the ratio between the peak integrals for each spectrum. Comparing these experimental peak integral ratios with the theoretical peak integral ratios provides a percentage error. Given more time in this experiment standard deviations could be calculated from thresholds on the peak integral ratios. The thermal state peak integrals were calculated to deviate by 1.5% from the expected value. The CNOT peak integrals and pure state peak integrals were calculated to each deviate by 20% from the theoretical expected values. The largest source of systematic error is the measurement of J.

5. CONCLUSIONS

The use of pulsed NMR to implement a two qubit quantum computer is demonstrated. Quantum operations are successfully performed by applying series of rotations to the each qubit. Pure initial states are constructed using temporal averaging on the thermal state of the system. The thermal state ratio of peak integrals deviate from the expected theoretical thermal values state by 1.5% and the pure state ratios differ by 20%. The pure initial states are used to demonstrate a CNOT gate that differs from the theoretical peak integral ratios by 20%. Using the CNOT gate, the Deutsch-Jozsa algorithm for determining balance of a single-bit function is performed for each of the four possible logical functions. The Deutsch-Jozsa algorithm is shown to behave as theoretically predicted.

[1] N. A. Gershenfeld and I. L. Chuang, Science (1997).

[2] I. L. Chuang and M. A. Nielsen, *Quantum Computation and Quantum Information* (Cambridge University Press, 2000).

[3] I. L. Chuang and L. M. K. Vandersypen, Nature (1998).

[4] N. Bloembergen, E. Purcell, and R. Pound, Phys. Rev. (1948).

[5] P. Bevington and D. Robinson, *Data Reduction and Error Analysis for the Physical Sciences* (McGraw-Hill, 2003).
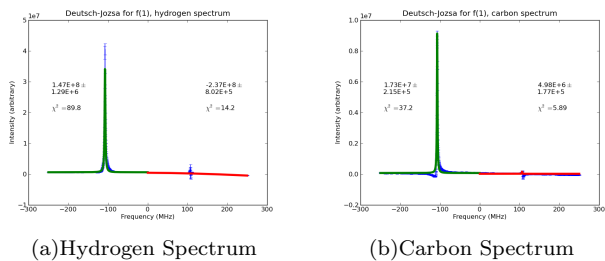
(a)Hydrogen Spectrum   (b)Carbon Spectrum

FIG. 6: The Deutsch-Josza algorithm acting on f_1, a constant function. The expected result is $|00\rangle$. The positive magnitude peak in each of the H and C spectra identify that the sample is in the state $|00\rangle$, confirming the hypothesis.
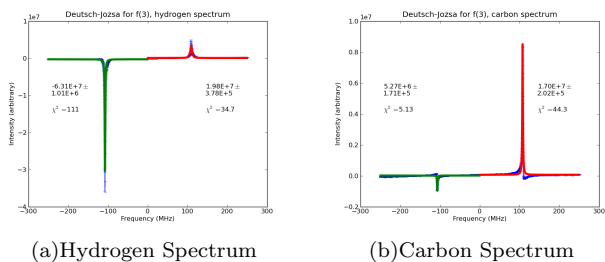

(a)Hydrogen Spectrum   (b)Carbon Spectrum

FIG. 7: The Deutsch-Josza algorithm acting on f_3, a balanced function. The expected result is $|10\rangle$. The negative magnitude hydrogen peak and positive magnitude carbon peak identify that the sample is in the state $|10\rangle$, confirming the hypothesis.